

## Odour-tracking capability of a silkmoth driving a mobile robot with turning bias and time delay

This article has been downloaded from IOPscience. Please scroll down to see the full text article.

2013 Bioinspir. Biomim. 8 016008

(<http://iopscience.iop.org/1748-3190/8/1/016008>)

View [the table of contents for this issue](#), or go to the [journal homepage](#) for more

Download details:

IP Address: 78.106.253.249

The article was downloaded on 08/02/2013 at 11:03

Please note that [terms and conditions apply](#).

# Odour-tracking capability of a silkworm driving a mobile robot with turning bias and time delay

N Ando, S Emoto and R Kanzaki

Research Center for Advanced Science and Technology, The University of Tokyo, Tokyo 153-8904, Japan

E-mail: [ando@brain.imi.i.u-tokyo.ac.jp](mailto:ando@brain.imi.i.u-tokyo.ac.jp)

Received 1 October 2012

Accepted for publication 10 January 2013

Published 5 February 2013

Online at [stacks.iop.org/BB/8/016008](http://stacks.iop.org/BB/8/016008)

## Abstract

The reconstruction of mechanisms behind odour-tracking behaviours of animals is expected to enable the development of biomimetic robots capable of adaptive behaviour and effectively locating odour sources. However, because the behavioural mechanisms of animals have not been extensively studied, their behavioural capabilities cannot be verified. In this study, we have employed a mobile robot driven by a genuine insect (insect-controlled robot) to evaluate the behavioural capabilities of a biological system implemented in an artificial system. We used a male silkworm as the 'driver' and investigated its behavioural capabilities to imposed perturbations during odour tracking. When we manipulated the robot to induce the turning bias, it located the odour source by compensatory turning of the on-board moth. Shifting of the orientation paths to the odour plume boundaries and decreased orientation ability caused by covering the visual field suggested that the moth steered with bilateral olfaction and vision to overcome the bias. An evaluation of the time delays of the moth and robot movements suggested an acceptable range for sensory-motor processing when the insect system was directly applied to artificial systems. Further evaluations of the insect-controlled robot will provide a 'blueprint' for biomimetic robots and strongly promote the field of biomimetics.

 Online supplementary data available from [stacks.iop.org/BB/8/016008/mmedia](http://stacks.iop.org/BB/8/016008/mmedia)

(Some figures may appear in colour only in the online journal)

## 1. Introduction

Autonomous robots capable of finding odour sources have become important in the detection of hazardous material spills or leaks in the environment. To track odour plumes and locate their source, odour-source localization requires the use of fine chemical sensors with high sensitivity, selectivity and short response/recovery time, as well as behavioural algorithms. Various algorithms have been proposed for odour source localization [1, 2], and those based on biological systems are among the most important approaches because the detection of odour sources is necessary for survival in organisms which have evolved unique behavioural strategies for tracking odours [3, 4].

Chemotaxis, the process of tracking of a chemical concentration gradient, is a fundamental behavioural strategy, and behavioural models based on model organisms, such as *Escherichia coli*, *Caenorhabditis elegans* and larvae of *Drosophila melanogaster*, have been proposed [4–8]. On the other hand, the search for odour sources in atmosphere requires additional strategies because odorants are intermittently distributed in the atmosphere [9, 10]; therefore, organisms cannot acquire a concentration gradient for simple chemotaxis. Insects are suitable models for the assessment of the strategy for tracking airborne odorants. Behavioural analyses in flying moths indicate that intrinsically programmed behaviour, upwind surge followed by sustained zigzag flight, is essential for contact with distributed clusters of odorants and is combined with other sensory feedbacks, such as mechanical

(flow direction) and visual information (optic flow), for successful localization [3, 11–14].

From a biomimetic perspective, a bottom-up approach is essential for the development of robots based on biological systems [15, 16]. In this approach, the behavioural model is based on research findings to date; thus, the accuracy of the model depends on the research progress. Among various model organisms, the study of the male silkmoth (*Bombyx mori*) is one of the best examples of bottom-up approaches because its characteristic odour-tracking behaviour and its neural basis are appropriately documented in neuroethological and robotic studies [17]. The male silkmoth responds to the conspecific female sex pheromone with a characteristic instinctive behaviour called mating dance, which includes wing vibrations, walking and abdominal curvature [18]. This walking behaviour is a well-defined programmed behaviour employed by the moth while searching for the pheromone source. Once the moth is stimulated by a single-puffed pheromone, it exhibits a stereotyped sequence of behaviour: surge (straight-line walking) and zigzagged walking consisting of several turns followed by a loop (a turn angle of more than 360°) [19]. This behavioural sequence is reset by an additional puff of pheromone stimulus; therefore, a moth stimulated by repeated pheromone puffs continues to perform straight-line walking. Behavioural studies also indicate that mechanisms involved in surges and zigzagged walking are different. A surge is a reflex action which lasts for the duration of the stimulus, while the subsequent zigzag and loop motions are self-generated behaviours which last even after the stimulus. Therefore, zigzag walking is considered to be a behavioural pattern which is similar to the self-generated zigzag flight of flying moths [14, 19]. Neurophysiological studies also report that these two behavioural properties are closely correlated with two types of neuronal activities in descending neurons, which convey motor commands from the brain to the thoracic motor centre [20–22]. The significance of this behavioural pattern for pheromone source localization has been confirmed by mobile robots, with real antennae acting as pheromone sensors [23, 24], which would also be the first step in the development of a biomimetic odour-tracking mobile robot.

In addition to the successful localization of an odour source, one would expect biological systems, especially sensory-motor systems responsible for animal behaviour, to be equipped with the capability of adaptive behaviour in constantly changing environments (adaptability), which is one of the most important attributes applicable to artificial systems, such as autonomous robots [17]. However, the bottom-up biomimetic study, which aims to obtain a complete behavioural model which in turn reconstructs the original behaviour of an animal, encounters two issues. First, we have not completely understood the behavioural capability, including the adaptability of the animal; therefore, the evaluation of the extent to which the current model can reconstruct the original behavioural capability is difficult. The other problem is that we are unaware of the method of application of the behavioural model to artificial systems, which exhibit different sensory-motor mechanisms from animals. Properties of artificial systems, such as time delay from the sensory input to the motor

output, sensitivity of sensors and manoeuvrability between animals and mobile robots, are not negligible. Therefore, we need to evaluate the necessity and method of modification of the model for robotic applications.

In the case of the silkmoth, even though the mobile robot implemented a model which can generate the rigid programmed behaviour for the location of the pheromone source [23, 24], the current model has not reconstructed the original behaviour of the moth. We have not implemented (presumably related to the adaptability) the convergence of pleural sensory-motor systems and its modulatory function to the programmed behaviour. Two sensory feedbacks have been assumed: bilateral olfactory information and visual information. Chemotactic directional control using bilateral olfactory inputs acquired by two antennae was confirmed by cutting or stimulating one antenna [18, 19]. High-speed video analysis indicates that the moth quantifies the concentration gradient using two antennae during a surge and walks towards the side with the highest concentration [25]. On the other hand, some descending neurons which are assumed to be involved in the pheromone-searching behaviour respond to optic flow stimuli [26]. Also, the neck motoneurons, which receive behavioural command signals from the descending neurons [20, 22], respond to both pheromone and optic flow stimuli [27]. The reported response to the optic flow corresponds to the optomotor response, which is a visually guided compensatory movement against involuntary displacement from a straight course [28]. We have observed that the walking moth shows an optomotor response to the optic flow stimuli, especially during a surge (in preparation). Although silkmoths possibly use these two sensory feedbacks for directional control, their effectiveness in realizing successful orientation remains unknown owing to experimental constraints. Either visual occlusion or ablation of the antennae is necessary when investigating their functions. However, walking insects with visual occlusion can exhibit the regular odour-tracking behaviour and localize the odour source [18, 29], and a decrease in the olfactory input by antennal ablation reduces the overall activity of the moth, preventing the moth from locating the source. Therefore, we believe that the application of perturbations to the intact sensory-motor system of the moth performing odour tracking is an effective way to investigate the ability of the moth to compensate for the perturbation with the sensory feedbacks.

Our technique employs an insect-controlled robot and manipulates its motor properties to generate perturbations in the sensory-motor feedbacks in intact insects. The robot is a two-wheeled robot driven by an on-board walking insect [17, 30], and it can track a pheromone plume and locate its source if a male silkmoth is used as the ‘driver’. We consider this robot as a single organism; the insect acts as the ‘brain’, while the robot acts as the ‘body’. Therefore, by manipulating the relationship between the insect and robot movements, the insect experiences unintentional movements, leading to its deviation from the correct course. If the moth can correct the course using the sensory feedbacks, then the robot would be able to successfully identify the pheromone source. A time delay can be set between the locomotion of

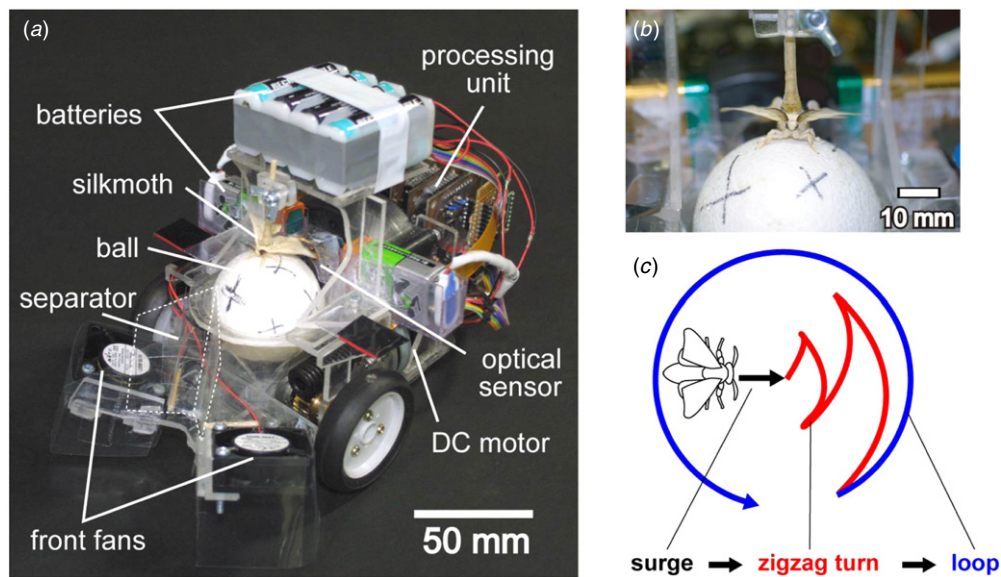


**Figure 1.** Insect-controlled robot and a male silkworm. (a) Insect-controlled robot. Dashed line indicates outline of a transparent separator for supplying airflow to each antenna. (b) A tethered moth on a ball. (c) Programmed behaviour of a male silkworm triggered by a single-puffed pheromone stimulus.

the on-board insect and the movement of the robot and the acceptable period of time spent for sensory-motor processing for successful localization can be investigated.

In this study, we first investigated the potential adaptability of the sensory-motor system in the silkworm. We manipulated the motor rotations of the robot to generate a turning bias (TB) towards one side and evaluated the insect's capability of overcoming this bias. Second, we set time delays between the insect locomotion and the corresponding robot movement to mimic the sensory-motor delay and determine the critical time precision required for successful localization. These evaluations would clarify the expected adaptability of the insect sensory-motor systems and provide us with useful information for applying the insect sensory-motor system to robotic odour tracking.

## 2. Materials and methods

### 2.1. Experimental animal

We used an adult male silkworm (*Bombyx mori*) aged two to eight days, which was either reared in our laboratory or purchased as a pupa. All larvae and pupas were reared at 27 °C, and adult moths were cooled at 15 °C one day after the eclosion to reduce their activities. Before the experiments, the moths were placed at room temperature (25–28 °C) for at least 10 min.

### 2.2. Insect-controlled robot

An insect-controlled robot (figure 1(a)) is a two-wheeled robot equipped with behavioural measurement, signal processing and motor control subsystems [30]. A male adult silkworm is tethered at the tip of a bar with an adhesive (G17, Konishi, Osaka, Japan), and it walks on a polystyrene ball, which is floated in air to reduce its friction (figure 1(b)). The

programmed behaviour of the moth triggered by a single puffed pheromone stimulus involves surge (straight-line, forward walking) and zigzagged walking motion (turning to the right and left), followed by a loop, as shown in figure 1(c). An optical mouse sensor (HDNS-2000, Agilent technologies, Santa Clara, CA) was positioned behind the ball to measure the walking-driven forward–backward and right–left rotations of the ball with a resolution of 0.254 mm at a sampling rate of 1500 Hz. An on-board microcontroller (ATMEGA8, Atmel, San Jose, CA) calculates the insect's trajectory from the sensor output and controls the rotation of two dc motors on opposite sides. The motors were driven by pulse width modulation at 1 kHz of the control cycle. We attached two 40 mm fans (1606KL-04W-B50, Minebea motor manufacturing, Tokyo, Japan) at the front of the robot to supply the air containing the pheromone to the on-board moth (flow speed: 2.0 m s<sup>-1</sup>) because the moth was placed at 90 mm height above the floor and was unable to receive the pheromone flowing on the floor. We think that the function of these fans is comparable to wing flapping of the walking silkworm during the pheromone tracking. The wing flapping generates airflow across its antennae in an anterior-to-posterior direction, which acts as 'sniffing' and enhances pheromone reception from wider area than the span of its antennae [31]. The airflows from these fans were separated by a separator to enhance the chemotaxis on the basis of bilateral olfactory cues (figure 1(a)).

### 2.3. Experimental conditions

**2.3.1. Wind tunnel.** We used a wind tunnel of size 1800 (L) × 900 (W) × 300 mm (H) for sex-pheromone source orientation tests at a wind speed of 0.7 m s<sup>-1</sup>. For the pheromone source, 2000 ng of a principle component of the female sex pheromone (synthetic bombykol: (E,Z)-10,12-hexadecadien-1-ol) dissolved in n-hexane and dropped on a piece of a filter paper was placed in a small cage (20 mm

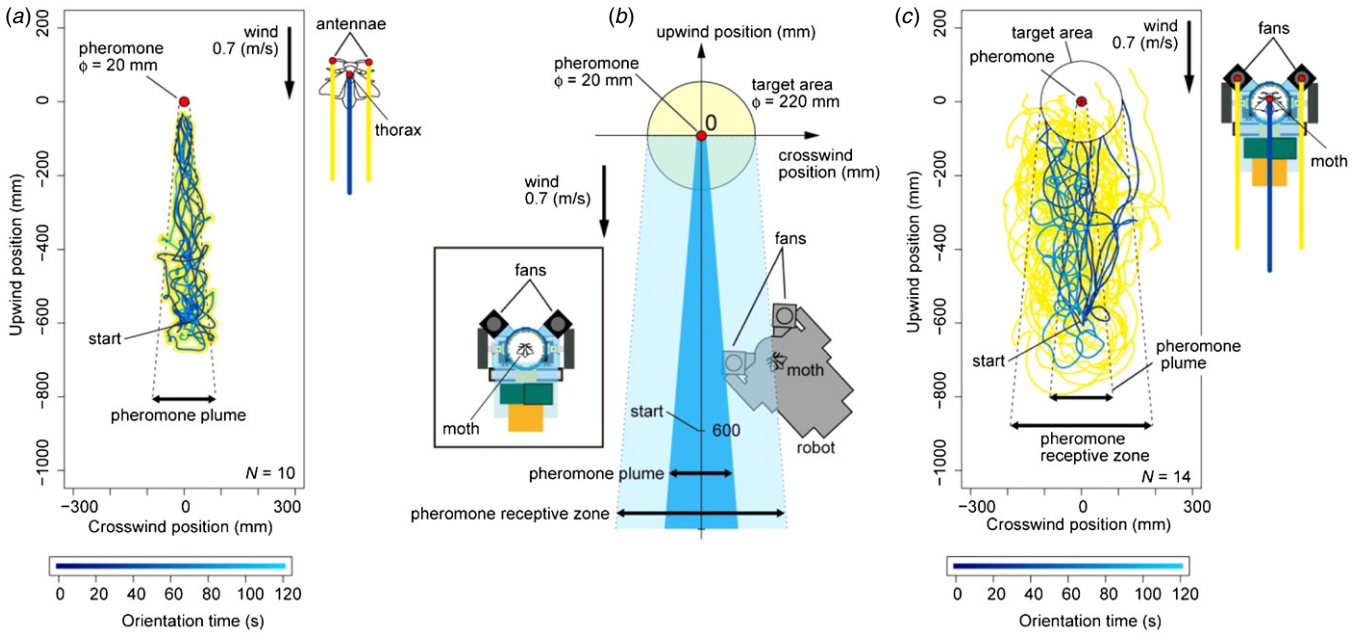


**Figure 2.** Comparison of pheromone tracking behaviours between the walking silkmoth and insect-controlled robot. (a) Trajectories of silkmoths during pheromone tracking. All ten moths located the source. Blue lines indicate the trajectories of moths and the orientation time in each trial is indicated by the colour strength. Yellow lines indicate the estimated trajectories of the antennae. Dashed lines indicate the estimated boundaries of the pheromone plume. (b) Definition of pheromone receptive zone (light blue), which is 200 mm wider than the pheromone plume (blue). (c) Trajectories of the robot during pheromone tracking. All trials driven by 14 moths located the source. Trajectories of the on-board moths and front fans are indicated by blue and yellow lines, respectively. Dashed lines indicate the boundaries of the pheromone receptive zone.

in diameter), which was placed on the floor upstream of the wind tunnel. For the visual cue, we displayed black and white grating patterns (interspacing: 30 mm) on the long sides of the walls in the wind tunnel. The orientation behaviour of the robot was filmed by a digital video camcorder at a frame rate of 30 Hz.

**2.3.2. Plume size and pheromone receptive zone.** The plume size was estimated by visualizing the airflow, using  $\text{TiCl}_4$  smoke. A superimposed image between the trajectories of ten silkmoths located the pheromone source (success rate of orientation was 100%), and the plume size indicated that all trajectories were in the plume (figure 2(a)). On the other hand, the distribution of the trajectories of the robot (position of the on-board silkmoth located at the centre between the two wheels) controlled by 14 silkmoths was broader than that of the plume (figure 2(c)), even though the robot achieved a success rate of 100% and there was no significant difference in orientation time between the walking silkmoth and the robot. This is because the robot takes the air containing the pheromone at 100 mm away from the moth with the two fans separated by 100 mm (the distance between centres of the two fans), while the walking silkmoth takes the air from the smaller area with the tiny antennae (around 6 mm long and attached onto the head with a 1 mm separation). Therefore, we set a ‘pheromone receptive zone’, which is 100 mm wider (corresponding to the distance between the on-board moth and the far end of the front fan) than the pheromone plume at each side, to visualize the zone in which the robot can receive the pheromone (figure 2(b)). Figure 2(c) shows that most of the

trajectories of the robot were distributed within the pheromone receptive zone.

**2.3.3. Manipulation of the robot.** To generate the TB, we amplified the forward rotation of the motor on one side and the backward rotation on the other side (figures 3(a) and (b)). This manipulation leads to an increase in the turn angular velocity in the ‘biased’ direction and also enables the robot to turn to the biased direction, even when the on-board moth walks in a straight line. The travel distance ( $\Delta L$ ) and turn angle ( $\Delta\theta$ ) per unit time ( $\Delta t$ ) of the robot are calculated on the basis of the travel distance of each wheel (figures 3(c) and (d)). The locomotion of the moth is detected as  $\Delta x$  for the right-to-left (clockwise-to-anticlockwise) direction and  $\Delta y$  for the forward-to-backward direction by the optical sensor. The travel distance of the wheels on the right and left sides ( $\Delta L_R$  and  $\Delta L_L$ ) are respectively described as

$$\Delta L_R = \Delta L_{R_x} + \Delta L_{R_y} \quad (1)$$

$$\Delta L_L = \Delta L_{L_x} + \Delta L_{L_y}, \quad (2)$$

where  $\Delta L_{R_x}$  and  $\Delta L_{L_x}$  are travel distances of the wheels on the right and left sides controlled by the clockwise-to-anticlockwise movements of the moth ( $\Delta x$ , turning), and  $\Delta L_{R_y}$  and  $\Delta L_{L_y}$  are those controlled by the forward-to-backward movements of the moth ( $\Delta y$ ). The positive values of  $\Delta x$  are the clockwise movements of the ball, and those of  $\Delta y$  are its forward movements (figure 3(c)). To generate TB, we changed the wheel rotation on each side by multiplying the gain values

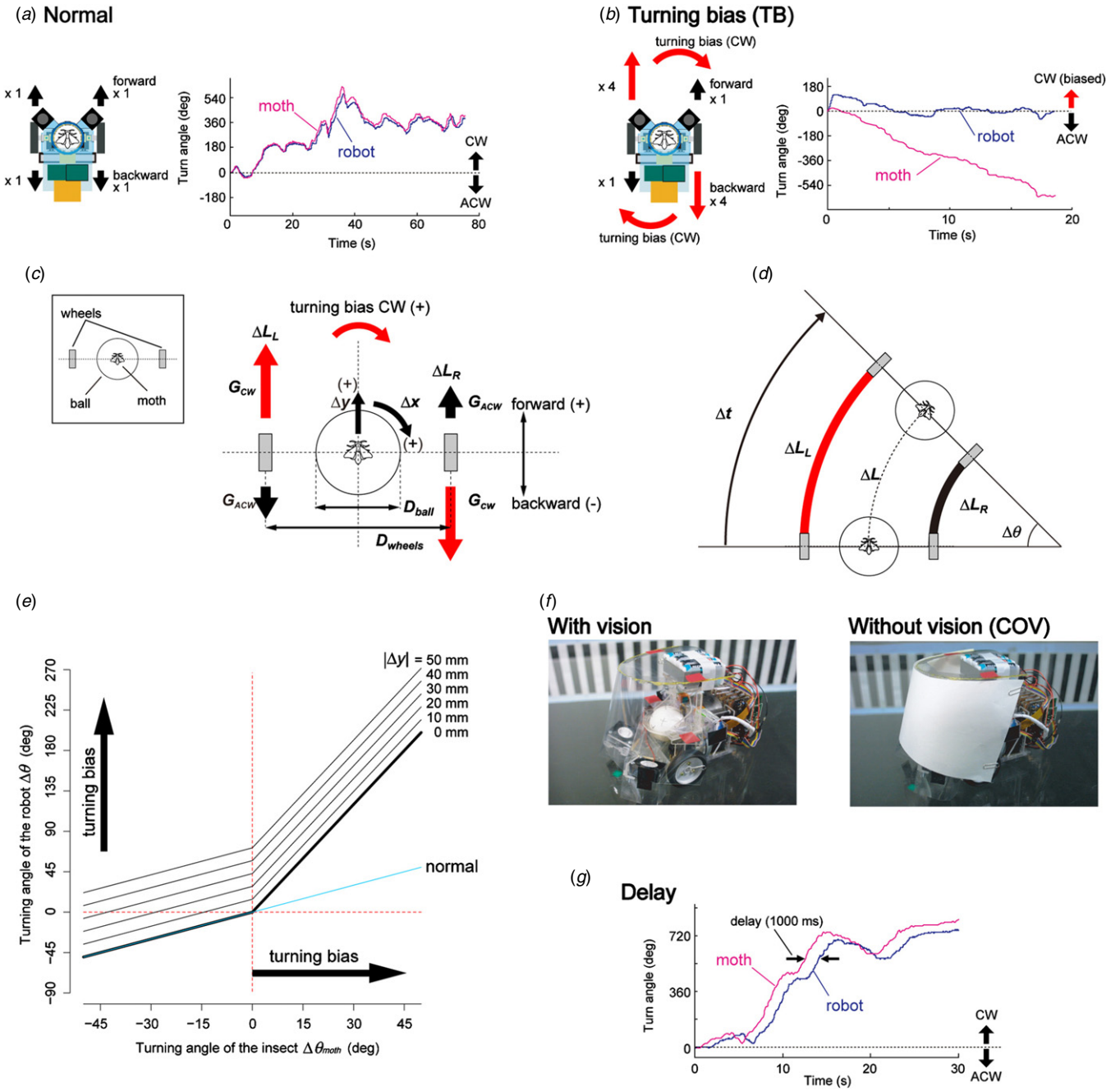


**Figure 3.** Manipulation of the insect-controlled robot. (a) Normal motor setting. Time course of turn angles between an on-board moth (magenta) and the robot (blue) during behaviour corresponded with each other. (b) Turning bias towards clockwise (CW) direction. Time course of turn angles indicates that anticlockwise (ACW) turning of the moth stabilized turn angle of the robot. (c), (d) Calculations of robot movement with the turning bias (see section 2). (e) Input–output characteristics of the turn angle with turning bias towards the clockwise direction, (black lines) and without turning bias (light blue line, normal). The characteristics with the turning bias differ in forward/backward (+/–) velocity of the moth. (f) Controlling visual field of the moth. (g) Time course of turn angles with time delay of 1000 ms (horizontal arrows) during odour tracking.

and the ball movements ( $\Delta x$ ,  $\Delta y$ ). The travel distances of the two wheels controlled by  $\Delta x$  are

$$\Delta L_{Lx} = -\Delta L_{Rx} = G_{CW} \Delta x \frac{D_{wheel}}{D_{ball}} \quad (\Delta x \geq 0: \text{clockwise}) \quad (3)$$

$$\Delta L_{Lx} = -\Delta L_{Rx} = G_{ACW} \Delta x \frac{D_{wheel}}{D_{ball}} \quad (\Delta x < 0: \text{anticlockwise}), \quad (4)$$

where  $G_{CW}$  is the gain required to increase or decrease the wheel rotation to realize clockwise turning of the robot,  $G_{ACW}$  is the corresponding gain for the anticlockwise turning,  $D_{wheel}$  is the distance between two wheels (120 mm) and  $D_{ball}$  is the diameter of the ball (50 mm). The travel distances of the wheels controlled by  $\Delta y$  are calculated as follows:

$$\Delta L_{Ly} = G_{CW} \Delta y, \quad \Delta L_{Ry} = G_{ACW} \Delta y \quad (\Delta y \geq 0: \text{forward}) \quad (5)$$

$$\Delta L_{Ly} = G_{ACW} \Delta y, \quad \Delta L_{Ry} = G_{CW} \Delta y \quad (\Delta y < 0: \text{backward}). \quad (6)$$

The travel distance ( $\Delta L$ ) per unit time ( $\Delta t$ ) for the robot is

$$\Delta L = \frac{\Delta L_L + \Delta L_R}{2} = \frac{\Delta L_{Ly} + \Delta L_{Ry}}{2} = \frac{(G_{CW} + G_{ACW})}{2} \Delta y. \quad (7)$$

Therefore, when the gains are  $G_{CW} = 4$  and  $G_{ACW} = 1$ , the travel distance of the robot ( $\Delta L$ ) is 2.5 times greater than that of the moth ( $\Delta y$ ). On the other hand, the turn angle of the robot ( $\Delta\theta$ ) is

$$\Delta\theta = \frac{\Delta L_L - \Delta L_R}{D_{\text{wheel}}} = \frac{\Delta L_{Lx} - \Delta L_{Rx}}{D_{\text{wheel}}} + \frac{\Delta L_{Ly} - \Delta L_{Ry}}{D_{\text{wheel}}} \quad (8)$$

$$= \Delta\theta_x + \Delta\theta_y,$$

where  $\Delta\theta_x$  and  $\Delta\theta_y$  are the turn angles of the robot determined by  $\Delta x$  and  $\Delta y$ , respectively. For each direction,  $\Delta\theta_x$  is calculated using (3) and (4) as

$$\Delta\theta_x = \frac{\Delta L_{Lx} - \Delta L_{Rx}}{D_{\text{wheel}}} = G_{CW} \frac{2\Delta x}{D_{\text{ball}}} \quad (9)$$

$$= G_{CW} \Delta\theta_{\text{moth}} (\Delta x \geq 0: \text{clockwise}),$$

$$\Delta\theta_x = \frac{\Delta L_{Lx} - \Delta L_{Rx}}{D_{\text{wheel}}} = G_{ACW} \frac{2\Delta x}{D_{\text{ball}}} \quad (10)$$

$$= G_{ACW} \Delta\theta_{\text{moth}} (\Delta x < 0: \text{anticlockwise}),$$

and for each direction,  $\Delta\theta_y$  is calculated using (5) and (6) as

$$\Delta\theta_y = \frac{\Delta L_{Ly} - \Delta L_{Ry}}{D_{\text{wheel}}} \quad (11)$$

$$= (G_{CW} - G_{ACW}) \Delta y (\Delta y \geq 0: \text{forward})$$

$$\Delta\theta_y = \frac{\Delta L_{Ly} - \Delta L_{Ry}}{D_{\text{wheel}}} \quad (12)$$

$$= -(G_{CW} - G_{ACW}) \Delta y (\Delta y < 0: \text{backward}),$$

where  $\Delta\theta_{\text{moth}}$  is the turn angle of the moth per unit time. Therefore, when the gains are  $G_{CW} = 4$  and  $G_{ACW} = 1$ , the robot turns in the clockwise direction, even though it moves straightforward or backward ( $\Delta x = 0$ ), and the turn angle ( $\Delta\theta_y$ ) increases with increasing  $\Delta y$ . The input ( $\Delta\theta_{\text{moth}}$ ) and output ( $\Delta\theta$ ) relationship for gains of  $G_{CW} = 4$  and  $G_{ACW} = 1$  is shown in figure 3(b). In this study, these gains were  $G_{CW} = 1$  and  $G_{ACW} = 1$  in a normal setting (figure 3(a) and movie S1 in supplementary data (available from [stacks.iop.org/BB/8/016008/mmedia](http://stacks.iop.org/BB/8/016008/mmedia))), while they were  $G_{CW} = 4$  and  $G_{ACW} = 1$  or  $G_{CW} = 1$  and  $G_{ACW} = 4$  for the TB (figure 3(b) and movie S2 in supplementary data). To investigate the function of visual information required for successful orientation, the on-board moth was surrounded by a transparent (with vision) or white sheet (covered: COV, without vision) (figure 3(f)). We combined the manipulations of the TB and vision and conducted the experiments for different conditions termed as CONT (normal motor setting with vision), COV (normal motor setting without vision), TB (turning bias with vision) and TB + COV (turning bias without vision). The orientation behaviours of the robot in CONT and TB are shown in movie S3 in the supplementary data.

The time delay between the locomotion of the on-board moth and the robot movement was achieved by storing locomotion data of the moth and playing them back as the robot movement after arbitrary time delays (movie S4 in

supplementary data). In this study, we set the time delays at 200, 400, 600, 800 and 1000 ms. The robot has an internal time delay of 200 ms to attain the maximum speed [30]; therefore, the actual time delays are set values plus up to 200 ms. The time-varying turn angles of the moth and robot for a time delay of 1000 ms are shown in figure 3(g).

**2.3.4. Pheromone source orientation.** In all trials, the start position was 600 mm downstream of the pheromone source, and the initial heading of the source was  $0^\circ$  (towards the pheromone source). The success of orientation was determined when the position of the on-board moth entered into the target area of 220 mm diameter within 210 s (figure 2(b)). On the other hand, if the robot could not locate the pheromone source within 210 s, or if it hit a wall of the wind tunnel, we considered that the trial was unsuccessful. The success rate of the orientation was calculated as the number of successful trials divided by the total number of trials. Each moth performed two trials (CONT and COV or TB and TB + COV) in the gain manipulation test (figures 4–8), one trial in the switching test (figure 9) and five trials of different delays in the delay test (figures 10 and 11).

**2.3.5. Data analysis.** The robot movements filmed by the video camera were captured on a computer. The position and heading of the robot on each frame were detected using a custom-made program written in Java. These time series data were then smoothed with a Gaussian window (bandwidth: 0.5 s). To evaluate the orientation behaviour of the robot, we focused on turning. To detect turns from trajectories of the robot, we defined a ‘turn’ as the turn of the robot in a given direction for more than 0.5 s (turn duration  $> 0.5$  s) at a turn angular velocity of more than  $5 \text{ deg s}^{-1}$ , and the turn angle for the duration was greater than  $30^\circ$ . The above definition does not indicate the discrimination of the zigzag turn of the programmed behaviour; instead, it indicates the detection of the consecutive (presumably voluntary or induced) turning behaviour during orientation. Therefore, these thresholds of turning parameters were considerably lower than the mean values of those in the zigzag turn of the programmed behaviour [19]. If the robot did not perform any detectable turns on the basis of the definition, we considered the turn duration, turn angular velocity and turn angle in the trial to be zero.

The walking behaviours of the moth were calculated from the ball rotations ( $\Delta x$ ,  $\Delta y$ ) stored on the on-board flash memory (sampling rate: 5 Hz). On the basis of the definition of ‘turn’, we detected the turns and calculated the turn duration, turn angular velocity and turn angle (product of turn duration and angular velocity).

We conducted statistical tests for comparisons between samples at a significance level of  $P < 0.05$ . Also, we used Fisher’s exact test with Bonferroni correction to compare the success rate; the Mann–Whitney U-test and Steel–Dwass test were used to compare two and multiple samples, respectively, while the Wilcoxon signed-rank test was used for comparisons of variables within the same individuals. We used R 2.14.2 [32] for data analyses and statistical tests.

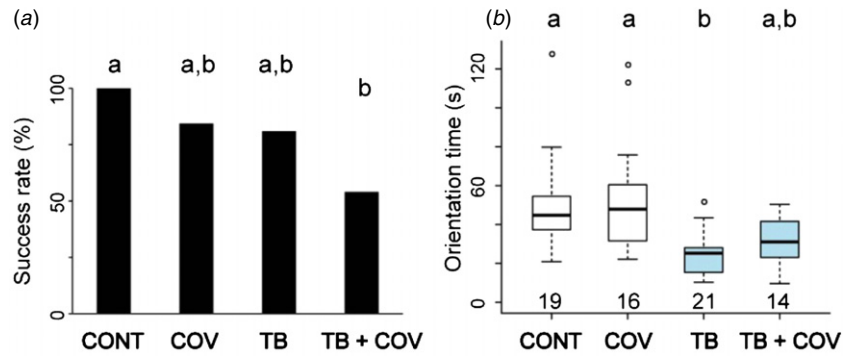


**Figure 4.** Orientation performance of the robot under four different conditions. (a) Success rates of orientation. (b) Orientation time. The numbers below boxes represent the number of successful trials. Plots with different letters indicate significant differences between them ( $P < 0.05$ ). CONT: control, COV: covered, TB: turning bias, TB + COV: turning bias with covered conditions.

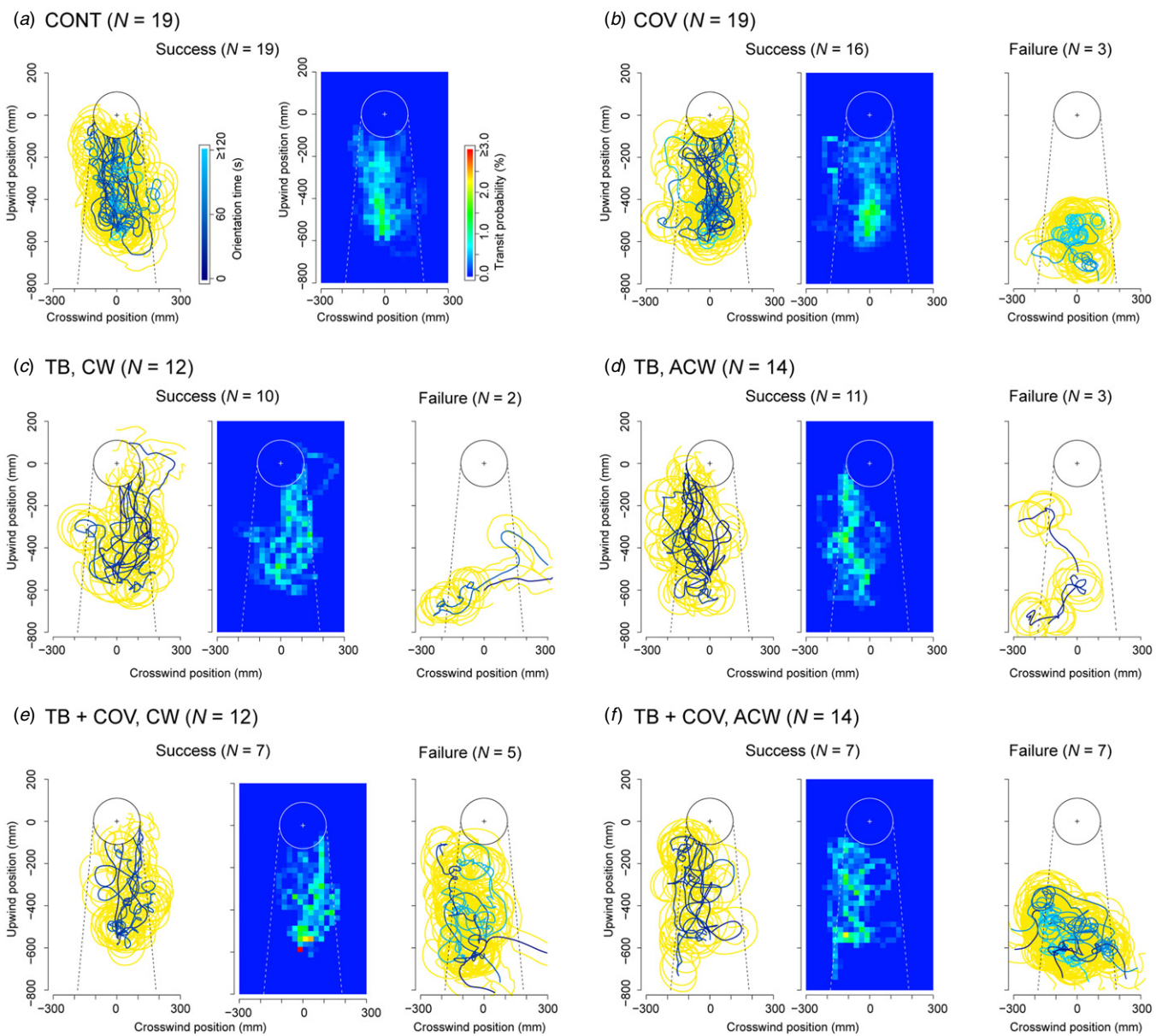


**Figure 5.** Trajectories and density plots of the transit probability during orientation. (a) Control, (b) covered, (c) turning bias for clockwise, (d) anticlockwise rotations, (e) turning bias towards clock rotation and (f) anticlockwise with covered conditions. Descriptions in trajectories (successful and failed trials) are the same as in figure 2(c). Density plots indicate the colour-coded transit probability (%), which is the time spent at each mesh (25 mm  $\times$  25 mm) divided by the sum of the orientation time of all succeeded trials.

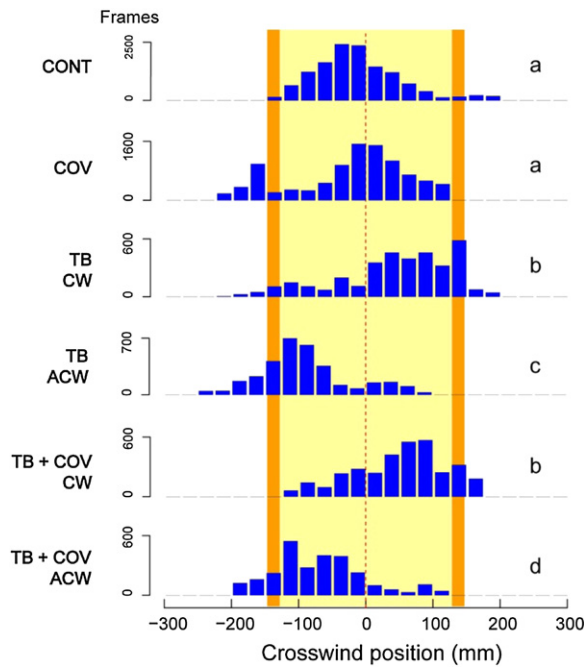


**Figure 6.** Histograms of time spent at each crosswind position within upwind positions from  $-200$  to  $-400$  mm (also see figure 5). The unit of the vertical axis is the number of frames (1 frame =  $1/30$  s). The pheromone receptive zone and its boundaries along the crosswind direction are coloured yellow and orange, respectively. The red dashed line indicates the centre of the pheromone receptive zone. Histograms with different letters indicate significant differences between them (Steel–Dwass test,  $P < 0.05$ ).

### 3. Results

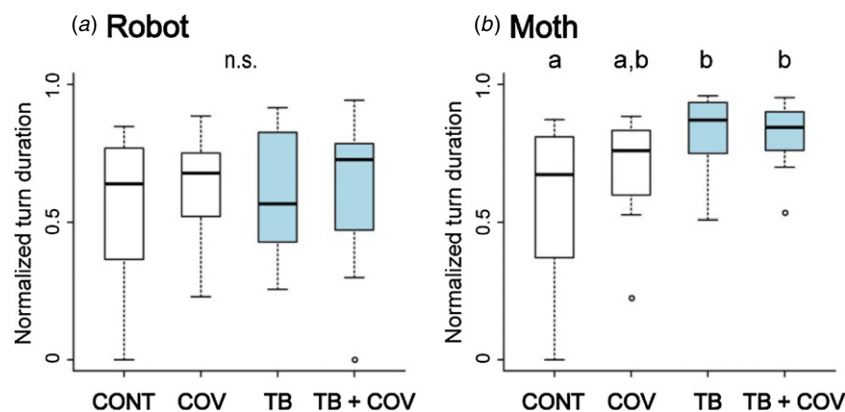
#### 3.1. Compensatory turning against the turning bias during pheromone tracking

Figure 4(a) shows the success rates under four different conditions. For the normal (non-manipulated) setting of the motor control, the robot achieved a success rate of 100% in control trials (CONT,  $N = 19$ ), and 84.2% when the visual field was covered by a white paper (COV,  $N = 19$ ). With the manipulation of the turning bias, the robot achieved a success rate of 80.8% without the covering (TB,  $N = 26$ ) and

53.8% with the covering (TB + COV,  $N = 26$ ), which was significantly lower than the success rate of CONT ( $P < 0.001$ , Fisher’s exact test with the Bonferroni correction). Successful trials with the manipulated conditions (TB and TB + COV) showed a shorter orientation time compared to that of non-manipulated conditions (CONT and COV), and there were significant differences in the orientation times for TB and two non-manipulated conditions (figure 4(b); Steel–Dwass test,  $P < 0.01$ ). These results indicate that the robot with the TB has a capability to localize the pheromone source with a high success rate and short orientation time, while the capability is affected by visual information.

The trajectories and density plots of the transit probability show the robot localized at the centre of the pheromone receptive zone in both CONT and COV trials (figures 5(a) and (b)). On the other hand, the robot with the turning bias (TB and TB + COV) followed the boundaries of the pheromone receptive zone; the robot with clockwise TB followed the boundary on the right side (figures 5(c) and (e)), while with anticlockwise turning, it followed the boundary on the left side (figures 5(d) and (f)). Distributions of the time spent along the crosswind direction in TB and TB + COV shifted to the boundaries of the pheromone receptive zone (figure 6) and there were significant differences in the crosswind positions between the manipulated (TB and TB + COV) and non-manipulated conditions (CONT and COV; Steel–Dwass test,  $P < 0.05$ ). These results indicate that the robot with the TB tracks a boundary of the pheromone receptive zone, which is necessary for successful localization to the odour source even without visual information.

The manipulation of the TB is expected to turn the robot towards the biased direction if the on-board moth does not compensate the TB. To examine the frequency with which the robot turned during orientation, we calculated the normalized turn duration, which is the sum of turn durations normalized by the orientation time in each trial. In the robot movements, there were no significant differences in the normalized turn durations between the manipulated and non-manipulated conditions (figure 7(a); Steel–Dwass test,  $P > 0.05$ ). On the other hand, the normalized turn durations of the moth under the manipulated conditions (TB and TB + COV) were significantly higher than that in CONT



**Figure 7.** Normalized turn durations of the robot (a) and on-board moths (b). Box plots with different letters indicate significant differences between them (Steel–Dwass test,  $P < 0.05$ ), and n.s. indicates differences that are not significant ( $P > 0.05$ ).

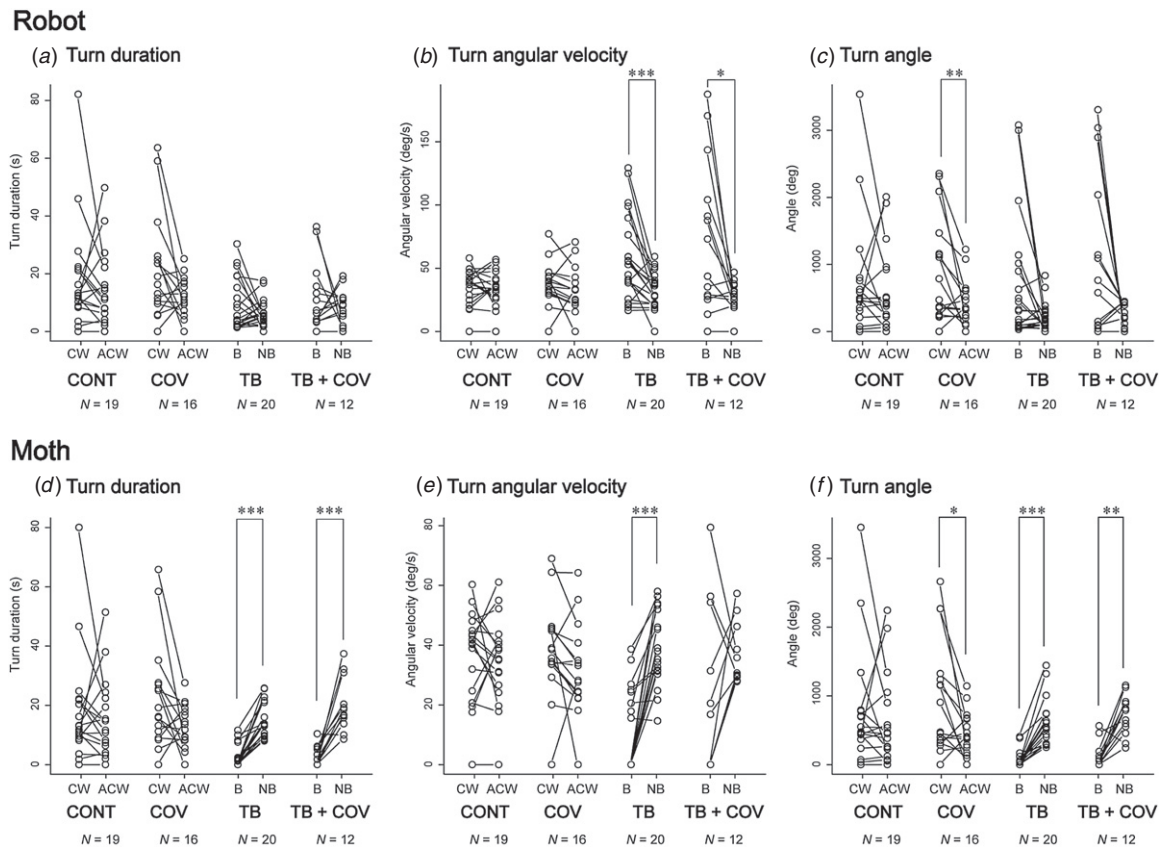


**Figure 8.** Directional preferences in turning parameters of the robot ((a)–(c)) and the on-board moth ((d)–(f)). The sum of the turn duration (a), (d), mean turn angular velocity (b), (e) and sum of the turn angle (c), (f) towards clockwise/anticlockwise (CW/ACW) or biased/non-biased directions (B/NB) in each trial are plotted with open circles linked by a line. The turns of the robot and the moth were independently detected based on its definition (see section 2). Significant differences in variables between directions are described as \* $P < 0.05$ , \*\* $P < 0.01$ , \*\*\* $P < 0.001$  (Wilcoxon signed-rank test).

(figure 7(b),  $P < 0.05$ ). This result indicates that the moth frequently performs turns in response to the manipulation, which may reduce the effect of the TB of the robot.

To clarify whether the on-board moth compensated the TB, we investigated its turn preference in each direction. Figure 8 shows the turn duration, turn angular velocity and turn angle of the robot and the moth for each turn direction (clockwise/anticlockwise and biased/non-biased directions). In the normal motor rotation (CONT and COV), there were no significant differences in the turning parameters of the robot between clockwise and anticlockwise directions (figures 8(a)–(c), Wilcoxon signed-rank test,  $P > 0.05$ ), except for the turn angle in COV (figure 8(c),  $P < 0.01$ ). With the TB, although there were no significant differences in the turn durations and angles of the robot between the biased and non-biased directions (figures 8(a) and (c),  $P > 0.05$ ), turn angular velocities towards the biased direction were significantly higher than those in the non-biased direction (figure 8(b),  $P < 0.001$  in TB and  $P < 0.05$  in TB + COV). On the other hand, for the turning behaviour of the moth (figures 8(d)–(f)), the overall turn preferences in TB and TB + COV were in opposition to those of the robot movements shown in figures 8(a)–(c). The turn durations for the non-biased direction were significantly longer than those for the biased direction in TB and TB + COV (figure 8(d),  $P < 0.001$ ). Furthermore, the moth did not

perform identifiable turns towards the biased direction in 10 of 20 trials in TB and 6 of 12 trials in TB + COV. The turn angular velocity for the non-biased direction was significantly higher than that for the biased direction in TB (figure 8(e),  $P < 0.001$ ) while not in TB + COV ( $P = 0.11$ ). The turn angles of the non-biased direction were significantly larger than those of the biased direction in both TB and TB + COV (figure 8(f),  $P < 0.001$  in TB and  $P < 0.01$  in TB + COV). These results indicate that the on-board moth has a preference for turning towards the non-biased direction and compensates the TB.

### 3.2. Transitional behavioural response to the manipulation

To elucidate whether the observed turning preference against the TB of the on-board moth could be induced by emergent manipulation of the motor settings, we investigated the ‘onset’ behavioural response of the moth by switching the motor control of the robot from CONT to TB during plume tracking.

Switching from CONT to TB was automatically triggered when the robot reached within 300 mm of the pheromone source with its heading within  $\pm 45^\circ$  relative to the direction of the source (figures 9(a) and (b)). We ended each trial when the robot was 150 mm away from the source with its heading within  $\pm 45^\circ$  relative to the source direction. After the switching (figure 9(c), red dashed line), the

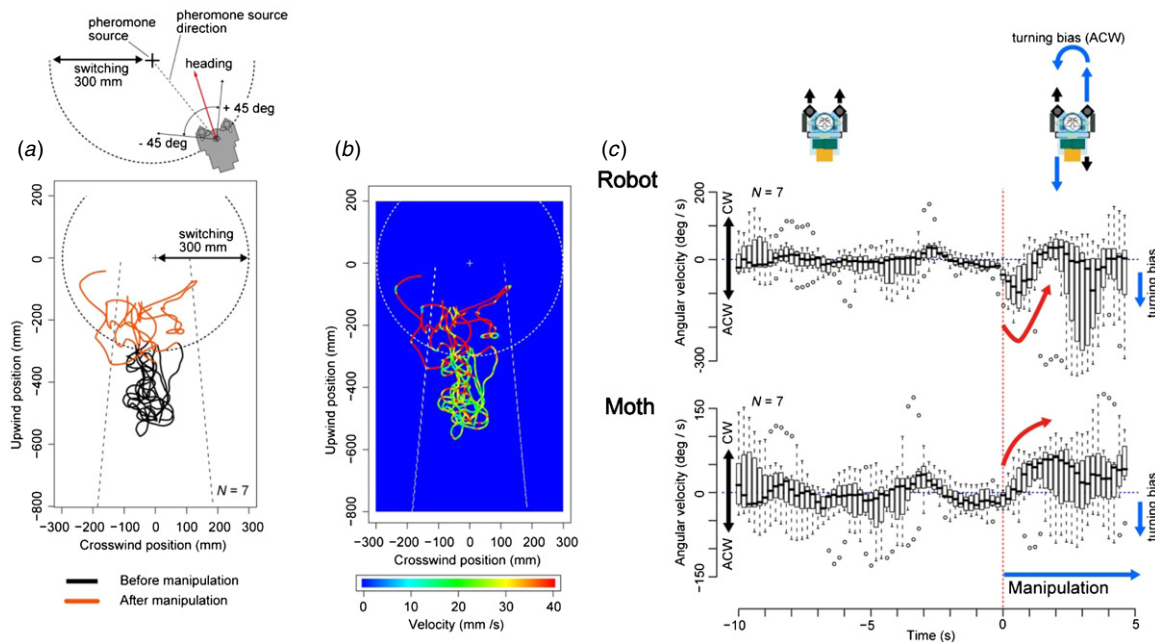


**Figure 9.** Switching the motor control from CONT to TB during orientation. (a) Procedure for the switching (top) and trajectories of the robot before (black lines) and after (orange lines) the manipulation (bottom). The switching was applied when the robot reached within 300 mm of the pheromone source (dashed circle) with its heading (red arrow) within  $\pm 45^\circ$  relative to the pheromone source direction. (b) Forward velocity of the robot. After the switching, the velocity increased (red) by the manipulation (see (7) in section 2). (c) Time course of the turn angular velocity of the robot and the moth before and after manipulation. A red dashed line (time = 0 s) indicates the onset of the manipulation of TB (a blue horizontal arrow). Trends of the transient changes in the turn angular velocities are shown by red arrows.

turn angular velocity of the robot increased towards the biased direction (anticlockwise direction), while that of the on-board moth increased towards the non-biased direction (clockwise direction), which reduced the turn angular velocity towards anticlockwise direction of the robot within 2 s (figure 9(c), indicated by red arrows). Comparisons of the turning parameters between the contralateral sides *after* the manipulations showed the similar tendency to figure 8: the turn duration and turn angle of the moth towards the non-biased direction *after* the manipulation were significantly larger than those towards the biased direction (figure S1 in supplementary data; Wilcoxon signed-rank test,  $P < 0.05$ ). These results indicate that the moth is able to change its turning behaviour in response to the TB and perform compensatory turning against it.

### 3.3. Limit of sensory-motor time delay for successful localization

In addition to the manipulation of TB, we set a time delay between the insect locomotion and the subsequent robot movement to investigate the limit of the sensory-motor time delay for successful localization to the odour source.

Figure 10(a) shows success rates of the robot with time delays. The success rate of the robot with the normal motor control (NORM) decreased gradually with increasing time delay, but the robot achieved a success rate of 90% even at a time delay of 600 ms. On the other hand, the success rate of the robot with the TB dropped sharply to 50% for a time delay of 400 ms. The orientation time of TB without the time delay was significantly shorter than that of NORM, which was also

seen for the time delay of 200 ms (figure 10(b); Mann–Whitney U-test,  $P < 0.01$ ). The normalized turn durations of the moth in NORM were significantly shorter than those of TB for time delays of 0 and 200 ms (figure 10(c),  $P < 0.001$  at 0 ms and  $P < 0.01$  at 200 ms), while there were no significant differences in the time delays between NORM and TB for relatively longer time delays, except at 800 ms ( $P > 0.05$ ; 400, 600 and 1000 ms). As the time delay increased, the trials in NORM tended to exhibit complicated trajectories with a number of turns (figure 11(a)), and the medians of the turn angle increased with increasing time delay (figure 11(b)), while this tendency was not observed in trials with TB (figure 11(d)). The robot with TB followed a boundary of the pheromone receptive zone on each side when the time delay was 0 ms (figure 11(c); see also the same condition shown in figures 5 and 6). However, the shift of tracking trajectories to the boundaries became obscure with increasing time delay. These results indicate that there is a limit of time delay (200 ms) for behaving normally and for compensation of the TB, while the time delays of up to 600 ms are acceptable for the robot in NORM to localize the odour source.

## 4. Discussion

### 4.1. Manipulation of the insect-controlled robot for exploring its potential capability

The pheromone-triggered programmed behaviour plays a dominant role in pheromone source orientation. Therefore, the evaluation of the involvement of the other sensory-motor systems in successful orientation has been difficult,

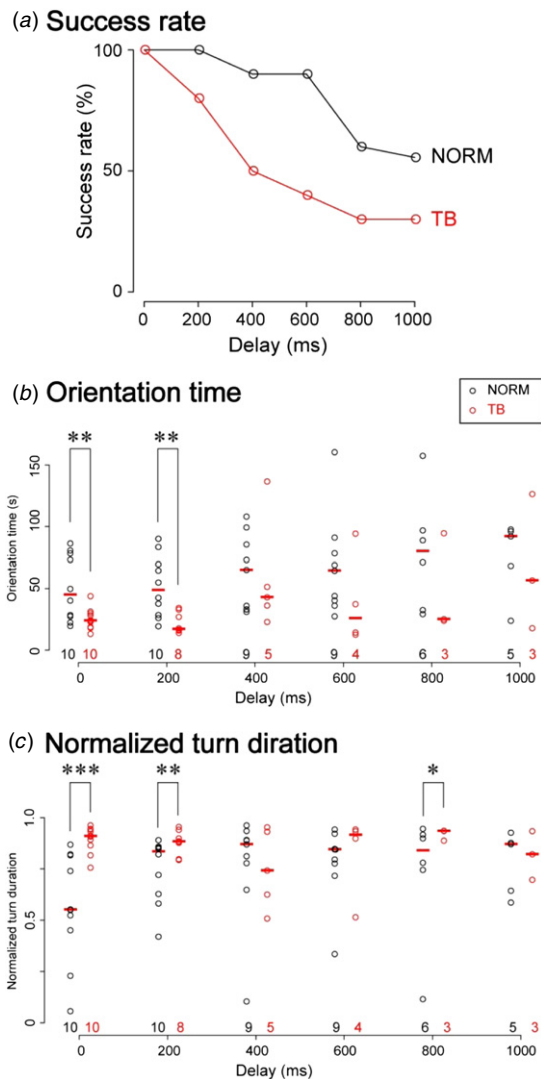


**Figure 10.** Effect of the time delay on orientation performance. (a) Success rates of the robot with the normal motor control (NORM, black) and the turning bias (TB, red). Each moth performed orientation for one (delay = 0 ms) or five times (delay = 200–1000 ms). The number of trials for each time delay was ten, except for a time delay of 1000 ms in NORM in which we excluded one trial because the moth ceased to behave within 20 s in the pheromone receptive zone due to low activity. (b) Orientation time. The red horizontal bar in each plot indicates the median and the number below the plot indicates the number of successful trials. (c) Normalized turn duration of the on-board moth. Significant differences in variables between directions are described as  $*P < 0.05$ ,  $**P < 0.01$ ,  $***P < 0.001$  (Mann–Whitney U-test).

although each of them was expected to be important for course control. In this study, by employing the insect-controlled robot with the manipulation of the TB, we were able to put the moth into an extraordinary situation in which the moth was required to change its behaviour, using those sensory-motor systems for successful orientation. The manipulation of the TB of the insect-controlled robot is comparable to the genetic manipulation of the TB in *Caenorhabditis elegans* (bent-head mutant *unc-23*, [33]). Furthermore, this enables us to appropriately manipulate the bias quantitatively at arbitrary times.

Since the on-board moth was tethered and exposed to airflow generated by the front fans, its condition might not be normal even though the tethered walking is a conventional method for analysing insect locomotion [19, 20, 25] and the airflow direction is less effective for course control of the pheromone tracking of the silkworm than that of flying moths [25]. However, from a biomimetic perspective, the condition of the moth would not prevent us from understanding how the insect sensory-motor system behaves in the artificial system and whether the whole system including the insect has a capability that we expect. We also think that the original behaviour of the moth was sufficiently elicited on the robot under the experimental condition that we employed. The robot achieved the same performance as walking silkworms, which was evaluated with the success rate of localization (100%) and orientation time (no significant difference between them).

#### 4.2. Parallel use of two sensory-motor systems for compensatory turning

With the manipulation of the TB, the on-board moth showed a turning preference towards the non-biased direction (figures 8(d)–(f)). The same preference was also seen in the switching experiment (figures 9(c) and S1(b)), suggesting that the on-board moth changed its behaviour in response to the change of sensory information induced by the TB. The response to the switching of the motor rotation of the robot suggested that relatively fast sensory-motor systems modulated the odour-tracking programmed behaviour. We discuss the functions of the two plausible sensory-motor systems: positive chemotaxis by bilateral olfaction and optomotor response by optic flow.

The shifts of tracking trajectories of the robot with TB to the boundaries of the pheromone receptive zone (figures 5(c)–(f) and 6) were observed even in the covered condition (TB + COV), suggesting the contribution of bilateral olfaction. In the absence of TB (CONT and COV), the robot tracked the pheromone at the centre of the receptive zone (figures 5(a), (b) and 6), where the on-board moth could receive the highest concentration of pheromone by both antennae. On the other hand, at the boundaries of the pheromone receptive zone, the on-board moth would receive the asymmetrical intensity of the bilateral olfactory input with the front fans; the antenna on the inner side of the receptive zone received a higher concentration than that on the contralateral side and turned towards the higher side owing to positive chemotaxis. The direction of the TB was closely related to the side of the shift of trajectories. For example, the robot with a clockwise turning bias (TB, CW) moved along the boundary of the pheromone receptive zone on the right, where the moth would be expected to perform anticlockwise turning because the pheromone concentration on the left side was higher than that on the right (positive chemotaxis). Therefore, we speculated that the manipulated TB of the robot and the chemotactic TB of the on-board moth were balanced at the boundaries of the pheromone receptive zone. Failed trials with the turning bias (TB and TB + COV) showed that the robot lost the receptive zone at a position away from the pheromone source (figures 5(c)–(f)), where the

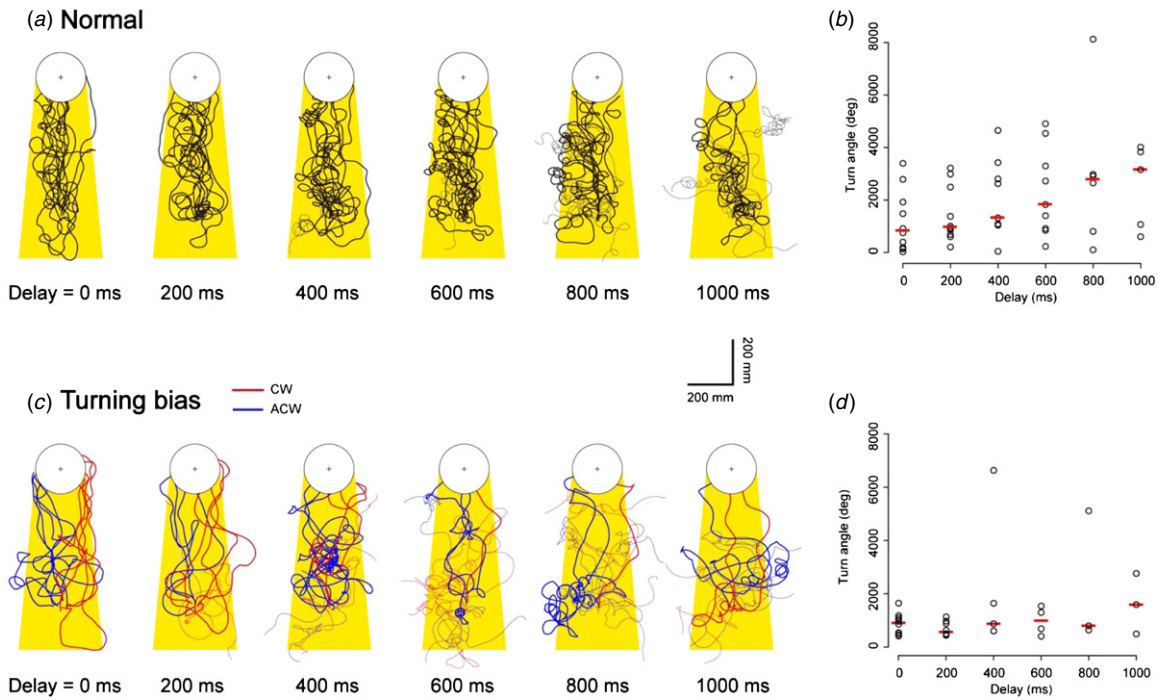


**Figure 11.** Orientation behaviour of the robot with time delays. (a) Trajectories of the robot with normal motor control. Trajectories shown by solid lines and dashed lines are successful and failed trials, respectively. The yellow areas indicate the pheromone receptive zone. (b) Turn angle (sum of the turn angles in both directions) of the robot with normal motor control. Red horizontal bars indicate medians. (c) Trajectories of the robot with the turning bias. Turning biases towards clockwise and anticlockwise directions are shown by red and blue lines, respectively. (d) Turn angle of the robot with the turning bias.

pheromone would be diffused, and the moth may not possess a sufficient concentration gradient to overcome the TB by bilateral olfaction. We also tested for relatively lower gains with the same ratio ( $G_{CW} = 2$  and  $G_{ACW} = 0.5$ ,  $G_{CW} : G_{ACW} = 4 : 1$ ) or with a lower ratio of gains ( $G_{CW} = 2$  and  $G_{ACW} = 1$ ,  $G_{CW} : G_{ACW} = 2 : 1$ ) (figures S2 and S3 in supplementary data [stacks.iop.org/BB/8/016008/mmedia](http://stacks.iop.org/BB/8/016008/mmedia)). These data also showed compensatory turning against turning biases (figure S3(d)–(f)), while shifts of trajectories to the boundaries were obscure, especially for the ratio  $G_{CW} : G_{ACW} = 2 : 1$  (figure S2(c) and (d)), which implied that the moth quantified a slight difference in the bilateral pheromone concentration in the plume. Further behavioural studies and characterization of the concentration distributions in the wind tunnel will clarify the effectiveness of bilateral olfaction.

Covering the visual field of the on-board moth reduced the success rate of orientation in both motor settings (figure 4(a)), and the TB + COV condition resulted in a significantly decreased success rate. On the other hand, other behavioural parameters between successful trials in TB and TB + COV were similar, with the only exception being the turning angular velocity (figure 8(e)). As indicated above, a decreasing success rate would be mainly due to failed trails in which the robot lost the pheromone plume away from its source, which was especially prominent under the covered condition (COV and TB + COV, figure 5(b) and (f)). Therefore, we hypothesized that the visual information was effectively involved in stabilizing the course control as an optomotor response until the moth encountered the concentration gradient of the pheromone, where it would be able to perform positive chemotaxis on the basis of bilateral olfaction. The

short orientation time in TB (figure 4(b)) is caused by the increasing forward/backward velocity of the robot owing to the TB (7), indicating that the manipulated TB was effectively compensated by the parallel use of the two sensory-motor systems.

#### 4.3. Temporal properties of the sensory-motor systems in odour tracking

The time delay of the motor response in the robot induces complex effects in the odour tracking. To ensure appropriate behaviour in constantly changing environments, reflexes and programmed behaviours of animals are triggered by specific sensory information and are presumably closely related to the timing and position of the sensory acquisition. On the other hand, in our experiment for the time delay, the behaviours of the robot became independent of sensory information with the increasing time delay of the motor response, which causes displacement of its own position and heading. Furthermore, the unintentional movement induced by the delayed motor response of the robot would be acquired as a ‘perturbation’ by the moth and would trigger additional behaviours in the attempt to compensate for the changes (the moth cannot fully compensate for any changes induced by the time delay).

The success rates, orientation time and normalized turn duration for time delays between 0 and 200 ms showed similar tendencies: high success rates and shorter orientation time in TB relative to that in NORM and a shorter normalized turn duration in NORM relative to that in TB (figure 10), which indicated that the acceptable range of time delay (presumably

**Table 1.** Estimations of displacements of the robot caused by time delays. B—biased direction; NB—non-biased direction; *N*—number of individuals. The displacements of the position and heading were estimated from the mean values of the forward and turn angular velocities.

NORM				
Delay (ms)	Success rate (%)	Displacement position (mm)	Heading (deg)	<i>N</i>
0	100	0	0	10
200	100	3.66	7.70	10
400	90	7.32	15.4	10
600	90	11.0	23.1	10
800	60	14.6	30.8	10
1000	55.6	18.3	38.5	9
TB				
Delay (ms)	Success rate (%)	Displacement position (mm)	Heading (deg)	<i>N</i>
0	100	0	0	10
200	80	9.15	30.8 (B), 7.70 (NB)	10
400	50	18.3	61.6 (B), 15.4 (NB)	10
600	40	27.5	92.4 (B), 23.1 (NB)	10
800	30	36.6	123 (B), 30.8 (NB)	10
1000	30	45.8	154 (B), 38.5 (NB)	10

within 200 ms) in which the robot could exhibit normal orientation behaviour was limited. Considering the internal time delay of the robot (up to 200 ms [30]), the limit of the time delay from the sensory input to the motor output would be less than 400 ms.

The steep decline of the success rates in TB relative to those in NORM (figure 10(a)) is mainly caused by differences in the displacement of the robot, which are in turn caused by the delayed motor response between these two conditions. For example, possible longitudinal displacements for time delays of 200 and 400 ms in TB were 9.15 and 18.3 mm, respectively (table 1; 2.5 times (1) of longitudinal displacement in NORM, estimated from mean forward velocity in NORM  $18.3 \pm 6.24 \text{ mm s}^{-1}$ , mean  $\pm$  SD), and the success rates at these time delays were 80% and 50%, respectively, which were in appropriate agreement with the success rates in NORM for time delays of 400–600 and 1000 ms, respectively. Possible longitudinal displacements and success rates in NORM for the time delays of 400–600 ms were 7.32–11.0 mm and 90%, while those for the time delay of 1000 ms were 18.3 mm and 55.6%. If the robot exits the pheromone receptive zone owing to a greater displacement of its position, it would not be expected to return to the plume and would eventually hit the wall or stop because the on-board moth cannot perform any behavioural activity without the pheromone.

On the other hand, although the estimated displacement of the heading increased with increasing time delay (table 1; estimated from mean turn angular velocity  $38.5 \pm 16.4 \text{ deg s}^{-1}$ , mean  $\pm$  SD), it would not be a major factor in the reduction of the success rate. According to the pheromone-searching behaviour of the silkmoth, the moth continues to walk in a straight line as long as it continues to receive the pheromone in the pheromone plume, while it begins to exhibit zigzag and loop behaviours once it loses the pheromone, especially at the boundaries of the plume [19]. During zigzag and loop motions, the moth changes its heading but rarely

moves its axis of rotation (spin turn); therefore, the moth stays in the plume even with displacements in heading until the axis has not been shifted by positional displacements. The tendency of the medians of the turn angle to increase with increasing time delay in NORM (figure 11(b)) suggested that the disturbance of the heading due to the time delay prevents the moth from heading directly towards the pheromone source with olfactory cues, but the robot can stay in the plume owing to the spin turns and may stochastically locate the source. If we focus only on successful orientation, an acceptable time delay for orientation can be extended to up to 600 ms (success rate of 90%, figure 10(b)) owing to this characteristic turning. On the other hand, in TB, a larger positional displacement would prevent the robot from staying in the plume and would result in lower success rates.

#### 4.4. Contribution silkmoth behaviour to robotic odour tracking

The TB experiment suggested the potential adaptability of the odour-tracking behaviour of the silkmoth. In real situations, the TB can be compared to the disorder of motor control in a robot. Our results indicated that positive chemotaxis due to the bilateral olfactory input and optomotor response would be able to compensate for possible TBs caused by the disorder. On the other hand, the delay experiment suggested the limit of the time delay in the motor response, which can be considered as a requirement for the application of the silkmoth-behaviour model to an odour-tracking robot. A time delay limit of 400 ms, which is comparable to the processing time of the sensor outputs for controlling motors, would not prevent the development of an artificial odour-tracking robot if we use the simple behavioural model; however, we must consider the temporal properties of chemical sensors because most of the chemical sensors provide a fast response but a slow recovery time, which lasts several tens of seconds [1, 34], while the neuronal activities of olfactory receptors (the electroantennogram) indicated a recovery time of less than 1 s [25]. The use of chemical sensors with slow recovery times would complicate the simultaneous and continuous sampling and tracking of odours for a robot employing the silkmoth model. Odours can be tracked by alternating between two phases, namely sample and move, which might be a solution. The sample phase would require sufficient time for recovery of the sensor output, and the movement during the ‘move’ phase must be less than the distance considered for ensuring high success rate, for example, 11.0 mm (the estimated positional displacement for a time delay of 600 ms in NORM, success rate of 90%; see table 1), if the robot is of the same size as the insect-controlled robot employed in this study. We believe that further evaluation of the behavioural capabilities of the insect-controlled robot will provide us with useful suggestions for the application of an insect behavioural model to artificial systems and strongly promote the field of biomimetics.

#### Acknowledgments

We are grateful to Dr Shigeru Matsuyama (University of Tsukuba) for providing the purified bombykol. This research

was supported by the Innovations Inspired by Nature Research Support Program from Sekisui Chemical Co., Ltd and a grant-in-aid for Young Scientist B from the Japan Society for the Promotion of Science (JSPS).

## References

- [1] Russell R A 2001 Survey of robotic applications for odor-sensing technology *Int. J. Robot. Res.* **20** 144–62
- [2] Kowadlo G and Russell R A 2010 Robot odor localization: a taxonomy and survey *Int. J. Robot. Res.* **27** 869–94
- [3] Vickers N J 2000 Mechanisms of animal navigation in odor plumes *Biol. Bull.* **198** 203–12
- [4] Gomez-Marin A, Duistermars B J, Frye M A and Louis M 2010 Mechanisms of odor-tracking: multiple sensors for enhanced perception and behavior *Front. Cell. Neurosci.* **4** 6
- [5] Berg H C and Brown D A 1972 Chemotaxis in *Escherichia coli* analysed by three-dimensional tracking *Nature* **239** 500–4
- [6] Pierce-Shimomura J T, Morse T M and Lockery S R 1999 The fundamental role of pirouettes in *Caenorhabditis elegans* chemotaxis *J. Neurosci.* **19** 9557–69
- [7] Iino Y and Yoshida K 2009 Parallel use of two behavioral mechanisms for chemotaxis in *Caenorhabditis elegans* *J. Neurosci.* **29** 5370–80
- [8] Gomez-Marin A, Stephens G J and Louis M 2011 Active sampling and decision making in *Drosophila* chemotaxis *Nature Commun.* **2** 441
- [9] Murlis J and Jones C D 1981 Fine-scale structure of odour plumes in relation to insect orientation to distant pheromone and other attractant sources *Physiol. Entomol.* **6** 71–86
- [10] Murlis J, Elkinton J S and Cardé R T 1992 Odor plumes and how insect use them *Annu. Rev. Entomol.* **37** 505–32
- [11] Baker T C and Kuenen L P S 1982 Pheromone source location by flying moths: a supplementary non-anemotactic mechanism *Science* **216** 424–6
- [12] Kuenen L P S and Baker T C 1983 A non-anemotactic mechanism used in pheromone source location by flying moths *Physiol. Entomol.* **8** 277–89
- [13] Willis M A and Arbas E A 1991 Odor-modulated upwind flight of the sphinx moth, *Manduca sexta* L *J. Comp. Physiol. A* **169** 427–40
- [14] Kaissling K E 1997 *Pheromone-Controlled Anemotaxis in Moths in Orientation and Communication in Arthropods* ed M Lehrer (Basel: Birkhäuser) pp 343–74
- [15] Webb B 2002 Robots in invertebrate neuroscience *Nature* **417** 359–63
- [16] Webb B, Harrison R R and Willis M A 2004 Sensorimotor control of navigation in arthropod and artificial systems *Arthropod Struct. Dev.* **33** 301–29
- [17] Kanzaki R, Ando N, Sakurai T and Kazawa T 2008 Understanding and reconstruction of the mobiligence of insects employing multiscale biological approaches and robotics *Adv. Robot.* **22** 1605–28
- [18] Kellogg V L 1907 Some silkmoth reflexes *Biol. Bull.* **12** 152–4
- [19] Kanzaki R, Sugi N and Shibuya T 1992 Self-generated zigzag turning of *Bombyx mori* males during pheromone-mediated upwind walking *Zool. Sci.* **9** 515–27
- [20] Mishima T and Kanzaki R 1998 Coordination of flipflopping neural signals and head turning during pheromone-mediated walking in a male silkmoth *Bombyx mori* *J. Comp. Physiol. A* **183** 273–82
- [21] Mishima T and Kanzaki R 1999 Physiological and morphological characterization of olfactory descending interneurons of the male silkmoth, *Bombyx mori* *J. Comp. Physiol. A* **184** 143–60
- [22] Wada S and Kanzaki R 2005 Neural control mechanisms of the pheromone-triggered programmed behavior in male silkmoths revealed by double-labeling of descending interneurons and a motor neuron *J. Comp. Neurol.* **484** 168–82
- [23] Kuwana Y, Nagasawa S, Shimoyama I and Kanzaki R 1999 Synthesis of silkmoth's pheromone-oriented behavior by a mobile robot with moth's antennae as pheromone sensors *Biosens. Bioelectron.* **14** 195–202
- [24] Kanzaki R, Nagasawa S and Shimoyama I 2005 Neural basis of odor-source searching behavior in insect brain systems evaluated with a mobile robot *Chem. Senses* **30** (Suppl. 1) i285–6
- [25] Takasaki T, Namiki S and Kanzaki R 2012 Use of bilateral information to determine the walking direction during orientation to a pheromone source in the silkmoth *Bombyx mori* *J. Comp. Physiol. A* **198** 295–307
- [26] Olberg R M 1983 Pheromone-triggered flip-flopping interneurons in the ventral nerve cord of the silkmoth, *Bombyx mori* *J. Comp. Physiol. A* **152** 297–307
- [27] Minegishi R, Takashima A, Kurabayashi D and Kanzaki R 2012 Construction of a brain-machine hybrid system to evaluate adaptability of an insect *Robot. Auton. Syst.* **60** 692–9
- [28] Götz K G 1968 Flight control in *Drosophila* by visual perception of motion *Kybernetik* **4** 199–208
- [29] Willis M A, Avondet J L and Zheng E 2011 The role of vision in odor-plume tracking by walking and flying insects *J. Exp. Biol.* **214** 4121–32
- [30] Emoto S, Ando N, Takahashi H and Kanzaki R 2007 Insect-controlled robot—evaluation of adaptation ability *J. Robot. Mechatronics* **19** 436–43
- [31] Loudon C and Koehl M A R 2000 Sniffing by a silkworm moth: wing fanning enhances air penetration through and pheromone interception by antennae *J. Exp. Biol.* **203** 2977–90
- [32] R Development Core Team 2012 *R: A Language and Environment for Statistical Computing* (Vienna: R Foundation for Statistical Computing) ISBN 3-900051-07-0 [www.R-project.org](http://www.R-project.org)
- [33] Pierce-Shimomura J T, Dores M and Lockery S R 2005 Analysis of the effects of turning bias in chemotaxis in *C. elegans* *J. Exp. Biol.* **208** 4727–33
- [34] Harvey D, Lu T-F and Keller M 2006 Odor sensor requirements for an insect inspired plume tracking mobile robot *Proc. IEEE Int. Conf. on Robotics and Biomimetics* pp 130–5